Adiabatic theory for binary-encounter-electron emission

D. H. Jakubassa-Amundsen
Physics Section, University of Munich, 85748 Garching, Germany

P. Kürpick
J. R. Macdonald Laboratory, Department of Physics, Kansas State University, Manhattan, Kansas 66506-2604

(Received 21 October 1996)

The electron-impact approximation for the ejection of target electrons by heavy, highly charged projectiles is modified in order to allow for a distortion of the initial state by the heavy perturber. Model calculations for ionization of H_2 by 0.5–0.6 MeV/amu Cu^{5+} impact show that the binary-encounter peak is considerably broadened when distortion effects are included. In general, this leads to a better agreement of the peak shape with experimental data than the conventional binary-encounter model. [S1050-2947(97)00207-2]

PACS number(s): 34.50.Fa

I. INTRODUCTION

The spectroscopy of binary-encounter (BE) electrons ejected in heavy-ion–atom collisions is presently a field of great interest, both experimentally and theoretically. Binary-encounter electrons are readily identified in the electron spectra in the case of not too small collision velocities v, since they form a peak located near an energy of $E_0 = 2v^2\cos^2\vartheta_f$ for electron emission into the forward hemisphere ($\vartheta_f \lesssim 60°$) with respect to the beam direction. In the case of highly charged projectiles anomalies in the electron spectra were discovered that revealed the close connection between the ejection of loosely bound electrons and the elastic scattering of free electrons by a strong perturber field [1]. These anomalies concern the inverse scaling of the binary-encounter peak intensity with the ionic charge of the projectile, which is most obvious at small ejection angles of the electrons and at low to moderate ionic charges [2–6]. Also, double-peak structures were found at certain emission angles, which could be related to the Ramsauer-Townsend structures in elastic electron-ion scattering [7–11]. All these effects gradually disappear, however, when the collision energy is increased.

For the theoretical interpretation of these electron spectra, the binary-encounter model and related theories are commonly in use. The basic concept of these theories is the description of the ionization process in terms of quasielastic scattering of the active target electron from the projectile field, implying that the final state of the electron is a projectile continuum eigenstate [12–16]. On the other hand, the interaction between electron and target is neglected in the scattering process; the only role of the target is to provide the momentum distribution of the electron in its initial state. Since these theoretical models are based on a zeroth-order perturbation theory in the target field, combined with the use of an undisturbed initial target eigenstate, they are only valid at high collision energies.

However, the measurement of binary-encounter peak structures usually requires moderate impact velocities, which, although high with respect to the orbiting velocity of the active target (valence) electron, are low with respect to the projectile nuclear charge or even the projectile ionic charge. Hence, while providing a qualitative explanation of the observed anomalies, the binary-encounter theories often fail to be in quantitative accord with the experimental data [9,10].

In this work a molecular perturbation theory is applied for the description of the binary-encounter electrons. In this theory, the target and the projectile potential are allowed to influence the electronic initial state. In a slow collision, the electron will follow a molecular orbital [17–20] as projectile and target are approaching each other, until ionization occurs at very small internuclear distances. When the collision is slightly more energetic, the electron may be transferred to adjacent molecular orbitals via Landau-Zener transitions [21,22] before it is ionized. In this case, electron ejection may be viewed as originating from a superposition of initial states weighted with the corresponding occupation probabilities, rather than originating from a single initial state. The shape of the binary-encounter peak will then be determined from the superposition of the momentum distributions of the populated molecular orbitals at the internuclear distance where ionization takes place.

This paper is organized as follows. In Sec. II, the electron-impact approximation [13], a quantal version of the binary-encounter model, is reformulated in terms of adiabatic perturbation theory. The molecular orbitals (MO) are provided by an ion-atom correlation diagram calculation, and their occupation numbers are evaluated within the Landau-Zener formalism. The results for the test systems 0.53 and 0.6 MeV/amu $Cu^{5+}+H_2$ are given in Sec. III. Scaling relations for the MO occupation numbers are found and, with their help, electron emission from 0.3 MeV/amu $Cu^{4+}+H_2$ collisions is calculated. For all these systems, comparison is made with available experimental data. The conclusion is drawn in Sec. IV. Atomic units ($\hbar = m = e = 1$) are used unless otherwise indicated.

II. THEORY

Our basic concern in this paper will be single target ionization, which means the ejection of one target electron while the projectile ion remains unaffected. For highly charged ions, electron loss will be quite unlikely because of

the strong binding as compared to the target valence electrons. On the other hand, the ejection of an energetic binary-encounter electron requires close collisions so that multiple-target ionization is strongly suppressed in the energy region of the binary-encounter peak. Therefore, the active electron can be described within the independent-particle model while the passive projectile and target electrons are accounted for by means of modified single-particle potentials and wave functions. Furthermore, the semiclassical approximation is used, representing the internuclear motion in terms of a classical trajectory.

A. Adiabatic electron-impact approximation

In the case of a strong perturber field, its influence on both the initial and final states of the active electron has to be treated nonperturbatively. For slow collisions (as compared to typical *projectile* electron orbiting velocities), the electronic states $\phi_i^{\rm MO}$ and $\phi_f^{\rm MO}$ are conventionally taken as eigenstates to the combined field V_P+V_T of projectile and target. This leads to the adiabatic perturbation theory where, to first order, the transition amplitude for electron emission is given by

$$a_{fi}=-\int dt\left\langle \phi_f^{\rm MO}(\vec{R})\left|\frac{\partial}{\partial t}\right|\phi_i^{\rm MO}(\vec{R})\right\rangle e^{i\int dt(\varepsilon_f^{\rm MO}-\varepsilon_i^{\rm MO})}. \quad (1)$$

The states $\phi_{i,f}^{\rm MO}$ as well as their energies $\varepsilon_{i,f}^{\rm MO}$ depend on time via the internuclear coordinate $\vec{R}$. Since we are concerned with the emission of binary-encounter electrons requiring close collisions with typical impact parameters $b\sim v/\Delta\varepsilon \sim(2v\cos^2\vartheta_f)^{-1}\lesssim v^{-1}$, we replace the molecular functions by their united-atom limit $\phi_{i,f}^{\rm UA}=\phi_{i,f}^{\rm MO}(R=0)$ and follow Briggs [23] to obtain

$$a_{fi}=-i\int dt\langle\phi_f^{\rm UA}|V_P+V_T|\phi_i^{\rm UA}\rangle e^{i(\varepsilon_f^{\rm UA}-\varepsilon_i^{\rm UA})t}. \quad (2)$$

For heavy perturber fields V_P as compared to the target field V_T (i.e., $Z_P\gg Z_T$ where Z_P and Z_T are the nuclear charges of projectile and target), V_T can be neglected in the transition operator as well as in the final state. This leads to the adiabatic electron-impact approximation (a-EIA)

$$a_{fi}=-i\int dt\langle\phi_f^P|V_P|\phi_i^{\rm UA}\rangle e^{i(\varepsilon_f-\varepsilon_i^{\rm UA})t}, \quad (3)$$

where now ϕ_f^P is an unbound projectile eigenstate. Equation (3) differs from the conventional EIA solely by the replacement of the initial target eigenstate with a bound eigenstate of the united atom formed by projectile and target. Therefore, the doubly differential cross section for the ejection of an electron with energy $\varepsilon_f=k_f^2/2$ into the solid angle $d\Omega_f$ is readily obtained from the EIA formalism [13,24]

$$\frac{d^2\sigma}{d\varepsilon_f d\Omega_f}(\phi_i^{\rm UA})=\frac{k_f}{v}\int d\vec{q}\ \delta(\varepsilon_f-\varepsilon_i^{\rm UA}+\vec{q}\cdot\vec{v}) \times|f_e(k,\theta)|^2|\varphi_i^{\rm UA}(\vec{q}+\vec{k}_f)|^2 \quad (4)$$

by introducing the Fourier transform $\varphi_i^{\rm UA}$ of the united-atom eigenstate. In the above expression, the on-shell approximation is made, and $f_e(k,\theta)$ is the amplitude for scattering a free electron elastically from the projectile field. Its momentum k and scattering angle θ are average values of the true electronic momenta in the initial and final states, $\vec{q}+\vec{\kappa}_f$ and $\vec{\kappa}_f$, respectively (in the projectile frame of reference, with $\vec{\kappa}_f=\vec{k}_f-\vec{v}$ and $\vec{k}_f$ the final-state momentum in the target frame). In all calculations, the Hartley and Walters on-shell prescription is used [25]:

$$k=\max(|\vec{q}+\vec{\kappa}_f|,\kappa_f),\quad \sin\frac{\theta}{2}=\frac{q}{2k}. \quad (5)$$

Equation (4) provides the ionization cross section when a single united-atom state is populated during the approach of the collision partners. If, however, several united-atom states are populated, the ionization cross section is obtained from a superposition,

$$\frac{d^2\sigma_{\rm tot}}{d\varepsilon_f d\Omega_f}=\sum_i P_i\frac{d^2\sigma}{d\varepsilon_f d\Omega_f}(\phi_i^{\rm UA}), \quad (6)$$

where P_i is the occupation probability of the state $\phi_i^{\rm UA}$. The calculation with probabilities rather than with amplitudes is not exact since interference terms are neglected. However, when the active electron is distributed over many molecular states, we expect that Eq. (6) is a reasonable approximation.

B. Population of the initial united-atom states

The population of electronic molecular states prior to ionization is conventionally obtained by solving the single-particle Dirac-Fock-Slater equations for the collision system in question [18–20]. In this formalism, the exact time-dependent electronic wave function is expanded in terms of molecular orbitals $\phi_n(\vec{r},\vec{R})e^{-i\int\varepsilon_n dt}$, which are eigenstates to V_P+V_T at a given internuclear separation R (for brevity, the superscript MO is dropped). This leads to a coupled system of differential equations for the expansion coefficients a_n:

$$\frac{d}{dt}a_n=-\sum_m a_m\left\langle\phi_n\left|\frac{\partial}{\partial t}\right|\phi_m\right\rangle e^{i\int(\varepsilon_n-\varepsilon_m)dt}, \quad (7)$$

where $\varepsilon_n(R)$ is the energy of $\phi_n(\vec{r},\vec{R})$. For later purpose, we note that the coupling matrix elements can be split into contributions from radial and rotational coupling,

$$\left\langle\phi_n\left|\frac{\partial}{\partial t}\right|\phi_m\right\rangle=\dot{R}\left\langle\phi_n\left|\frac{\partial}{\partial R}\right|\phi_m\right\rangle-i\dot{\theta}\langle\phi_n|\hat{j}_y|\phi_m\rangle, \quad (8)$$

with $\hat{j}_y=i\partial/\partial\theta$ the angular momentum operator. Since the adiabatic states ϕ_n are defined such that the magnetic quan-

tum number m_j is conserved, either radial coupling (for $\Delta m_j = 0$) or rotational coupling (for $\Delta m_j = 1$) does occur.

1. Calculation of the correlation diagram

Before solving Eq. (7), the relevant molecular orbitals and their energies have to be determined. Since the initial state of the active target (valence) electron has a small binding energy as compared to the electrons bound to the projectile nucleus, the separated-atom level of the active electron will correlate to high-lying, unoccupied states of the united atom formed by projectile and target. The correlation diagram is calculated with the relativistic Dirac-Fock-Slater linear combination of atomic orbitals–molecular orbital (LCAO-MO) basis set method as discussed in earlier work [18,20]. The time-independent Dirac-Fock-Slater equation containing nuclear, Coulomb, and exchange potentials,

$$[\hat{t} + \hat{V}^N(\vec{R}) + \hat{V}^C(\vec{R}) + \hat{V}_\alpha^{\mathrm{Ex}}(\vec{R})]\phi_n(\vec{r},\vec{R}) = \varepsilon_n(\vec{R})\phi_n(\vec{r},\vec{R}), \tag{9}$$

is solved by expanding $\phi_n(\vec{r},\vec{R})$ in a basis consisting of projectile ionic states ξ_ν^P and target atomic states ξ_μ^T:

$$\phi_n(\vec{r},\vec{R}) = \sum_{\nu=1}^{N_P} c_{n\nu}\xi_\nu^P(\vec{r},\vec{R}) + \sum_{\mu=1}^{N_T} d_{n\mu}\xi_\mu^T(\vec{r},\vec{R}). \tag{10}$$

The potentials involved in Eq. (9) are the electron-nucleus potential $\hat{V}^N(\vec{R})$, the electron-electron Coulomb potential $\hat{V}^C(\vec{R})$, and the Slater exchange potential $\hat{V}_\alpha^{\mathrm{Ex}}$ where the Slater parameter was set to $\chi_\alpha = 0.7$.

Figure 1 shows the correlation diagram for the test system $Cu^{5+} + H$. This is a simplification of the experimental system, $Cu^{5+} + H_2$, but it has been shown that for binary-encounter electron emission, the H_2 target (if not oriented) can well be approximated by two independent hydrogen atoms [10].

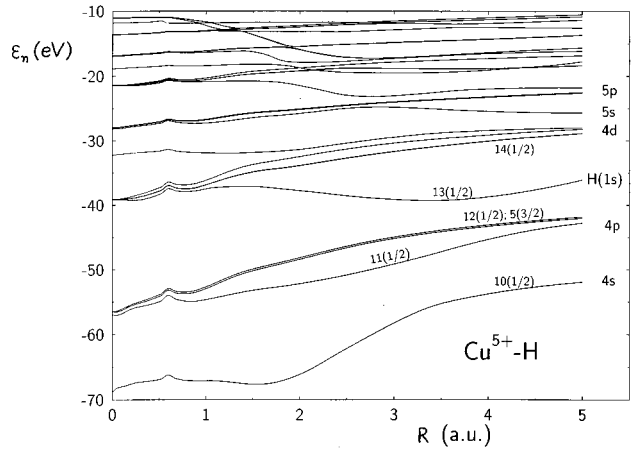

FIG. 1. Correlation diagram for the system $Cu^{5+} + H$. The lowest level shown is that of the 10(1/2) state connected to the UA $4s_{1/2}$ state, followed by 11(1/2), 12(1/2), and 5(3/2) connected to the UA $4p$ group. The levels adjacent to 13(1/2) [i.e., 14(1/2) +6(3/2) and 7(3/2)+2(5/2)] all relate to the UA $4d$ group whereas the subsequent 15(1/2) level connects to the UA $5s_{1/2}$ state. Only core states up to UA $4s_{1/2}$ are occupied by the Cu^{5+} electrons.

Included in the basis (10) are the projectile $1s_{1/2}$ to $6d_{5/2}$ states with angular momentum $l \leqslant 2$, as well as the target $1s_{1/2}$ to $2p_{3/2}$ states. All (separated-atom) projectile states $\{nlj\}$ that are more strongly bound than the hydrogen $1s_{1/2}$ state correlate to the corresponding $\{nlj\}$ states of the united atom. The target $1s_{1/2}(m_j = 1/2)$ ground state correlates via the $13(m_j = 1/2)$ molecular orbital to the UA $4d_{3/2}(m_j = 1/2)$ state, while for the higher-lying states, level promotion may occur. Since united-atom states are not included in the (truncated) basis set (10), one cannot expect the MO energies to converge to the exact UA energies in the limit $R \to 0$. However, the minor deviations for $R < 1$ do not affect the correlation of the various states.

2. MO coupling in the Landau-Zener formalism

As follows from Eq. (7), the time dependence of the two-center potential via $\vec{R}(t)$ induces couplings between the molecular-orbital states. If an isolated coupling between two molecular states is restricted to a small region ΔR around an avoided crossing point $\bar{R}$, the transition probability between these states can be obtained by means of the Landau-Zener formalism, a theory much simpler than a full time-dependent Dirac-Fock-Slater calculation. The application of this formalism requires, however, knowledge of the *diabatic* correlation diagram instead of the adiabatic correlation diagram shown in Fig. 1. This is achieved through a linear combination of the MO functions $\phi_n(\vec{r},\vec{R})$, or equivalently, through a transformation of their expansion coefficients a_n [17]:

$$a_n e^{-i\int \varepsilon_n dt} = \sum_k C_{nk}(R) b_k^{(d)}, \tag{11}$$

where $b_k^{(d)}$ are interpreted as expansion coefficients of the exact wave function in terms of the diabatic basis states. When Eq. (11) is inserted into the differential equations (7), a set of equations for $b_k^{(d)}$ is obtained. The transformation matrix C in Eq. (11) is found from the requirement that only potential (V) coupling occurs in these equations,

$$i\frac{\partial}{\partial t} b_k^{(d)} = \sum_m V_{km} b_m^{(d)}. \tag{12}$$

One obtains

$$\frac{\partial}{\partial t} C_{nk} = -\sum_{k'} \left\langle \phi_n \left| \frac{\partial}{\partial t} \right| \phi_{k'} \right\rangle C_{k'k}, \tag{13}$$

$$V_{km} = \sum_n C_{kn}^{-1} \varepsilon_n C_{nm},$$

where C^{-1} is the inverse matrix of C. If restriction is made to a two-level system ($n = 1,2$), one can readily solve for C and V [17]:

$$C=\begin{pmatrix} \cos\alpha & \sin\alpha \\ -\sin\alpha & \cos\alpha \end{pmatrix},$$

$$V=\begin{pmatrix} V_{11} & V_{12} \\ V_{12} & V_{22} \end{pmatrix}, \quad V_{11}=\varepsilon_1\cos^2\alpha+\varepsilon_2\sin^2\alpha, \quad V_{22}=\varepsilon_1\sin^2\alpha+\varepsilon_2\cos^2\alpha \quad V_{12}=\sin\alpha\,\cos\alpha(\varepsilon_1-\varepsilon_2) \tag{14}$$

with α defined through $\partial\alpha/\partial t=-\langle\phi_1|\partial/\partial t|\phi_2\rangle$. With the knowledge of the potential matrix V, the probability for remaining in the diabatic level i (with energy V_{ii}, coinciding at $R\to\infty$ with the *adiabatic* level i) or, equivalently, for *changing* from one *adiabatic* level i to the other one can be calculated within the Landau-Zener model. The diabatic levels have a real crossing at $\overline{R}$ [i.e., when $V_{11}(R)=V_{22}(R)$], and the transition probability from the (adiabatic) level 1 to level 2 is given by [21,22]

$$P_{1\to2}=e^{-\gamma}, \quad \gamma=2\pi|V_{12}|^2\left.\frac{1}{|\partial/\partial t(V_{11}-V_{22})|}\right|_{R=\overline{R}}, \tag{15}$$

whereas the probability for the electron to remain in level 1 is $P_{1\to1}=1-\exp(-\gamma)$ from the conservation of unitarity. The denominator of γ is proportional to $\partial\alpha/\partial t$ and hence to the adiabatic coupling matrix element $\langle\phi_1|\partial/\partial t|\phi_2\rangle$. For the radial respective rotational coupling one obtains

$$\gamma_{\rm rad}=\pi|\overline{\varepsilon_1}-\overline{\varepsilon_2}|/|4v_R\langle\phi_1|\partial/\partial R|\phi_2\rangle|_{\overline{R}}, \qquad \gamma_{\rm rot}=\pi|\overline{\varepsilon_1}-\overline{\varepsilon_2}|\overline{R^2}/|4bv\langle\phi_1|\hat{j}_y|\phi_2\rangle|_{\overline{R}}, \tag{16}$$

where $\overline{\varepsilon_i}=\varepsilon_i(\overline{R})$ are the adiabatic energies at the crossing point. Into the radial transition probability enters the radial velocity $v_R=v[1-(\overline{\varepsilon_1}+\overline{\varepsilon_2})/2E_{\rm c.m.}-(b/R)^2]^{1/2}$ (with $E_{\rm c.m.}$ the center-of-mass energy of the collision) such that both $\gamma_{\rm rad}$ and $\gamma_{\rm rot}$ depend on impact parameter b.

III. RESULTS

The doubly differential cross sections for binary-encounter-electron emission were calculated from the formula (6) with the initial-state occupation probabilities taken from Eqs. (15) and (16). For each electron spectrum, a fixed impact parameter $b=(2v\cos^2\vartheta_f)^{-1}$ was used to calculate the numbers P_i. For the calculation of the ionization cross sections (4), the elastic scattering amplitude was obtained by means of a partial wave expansion of the scattering state. The corresponding phase shifts were calculated numerically [24], using a static plus exchange potential for electron scattering from the copper ions: the static potential was obtained from a Hartree-Fock-Slater code taking the ground-state configuration of the Cu ions, and exchange was included via the local AAFEGE (asymptotically adjusted free-electron gas exchange) potential [26]. Polarization was neglected since it is not important for highly charged ions at large impact velocities. The united-atom energies and wave functions were obtained from a Dirac-Fock calculation, and their Fourier transforms $\varphi_i^{\rm UA}$ were found with the help of a fast Bessel transform routine [27,28].

A. The test system Cu^{5+} on H_2

We consider the two collision energies, 0.53 and 0.6 MeV/amu, corresponding to $v=4.6$ and 4.9 a.u., and emission angles ϑ_f between 0° and 40°. For the range of these parameters, we have $0.1\lesssim b\lesssim0.2$ a.u. From this it follows that the MO level couplings below $R=0.1$ are inaccessible and therefore the slight inaccuracies of the correlation diagram near $R=0$ do not play any role. We estimated the occupation probabilities from the coupling strengths between the initially occupied 13(1/2) state and the adjacent levels near $R\sim0.3$ (using the level energies ϵ_i and the adiabatic coupling matrix elements provided by the LCAO-MO calculation) and found that radial coupling was largely dominating. Couplings at larger distances R were neglected because many of them are weak or involve only intrasubshell coupling, and moreover, the couplings near $R\sim0.3$ are so strong that they would lead to a complete redistribution of probability anyway. Neglecting MO states for which the transition probability from the 13(1/2) state is much less than 10%, we have found that for the v and ϑ_f range considered above, the hydrogen electron during the approach of projectile and target is distributed over MO levels connecting to the following united-atom states $\phi_i^{\rm UA}$ with average probabilities P_i: $4p_{1/2}+4p_{3/2}$ (18%), $4d_{3/2}+4d_{5/2}$ (47.5%), $5s_{1/2}$ (10%), $5p_{1/2}+5p_{3/2}$ (14.5%), and $5d_{3/2}+5d_{5/2}$ (10%). These P_i values, which are normalized to 1, are quite insensitive to small changes in v or b. The deviation of the individual numbers for each group of states (i.e., when a fixed v and ϑ_f is selected) from the average numbers P_i given above is at most $\Delta P/P_i\sim6\%$ except for the $5p$ group at $v=4.6$ and $\vartheta_f=40°$ where one crossing is no longer reached (20%).

Figure 2 shows our results for 0.6 MeV/amu Cu^{5+} on H_2 at the emission angles 0°, 25°, and 40° in comparison with experimental data from Schmidt-Böcking and coworkers [10] recorded at the Heidelberg facilities. These earlier data are not measured on an absolute scale. We have therefore normalized them to the absolute data taken recently by Hagmann and collaborators [11,29] in Kansas. To this aim we have extrapolated the Kansas zero-degree data available for a variety of copper charge states and impact velocities to $v=4.9$ and charge state 5+ at the binary-encounter peak maximum to have a reference intensity for the Heidelberg data. When comparing these normalized 0° data to the conventional EIA theory it follows from Fig. 2(a) that although the experimental yield at the BE peak maximum is reproduced, the calculated peak width is too narrow and the intensity much too low for energies below the binary-encounter peak. The present a-EIA theory, although giving a smaller peak intensity, improves on the peak shape since the initial-state Compton profile (which determines the shape) is much wider for the (Cu^{5+}+H) UA $4d$ and the adjacent UA states than for the hydrogenic ground state used in the con-

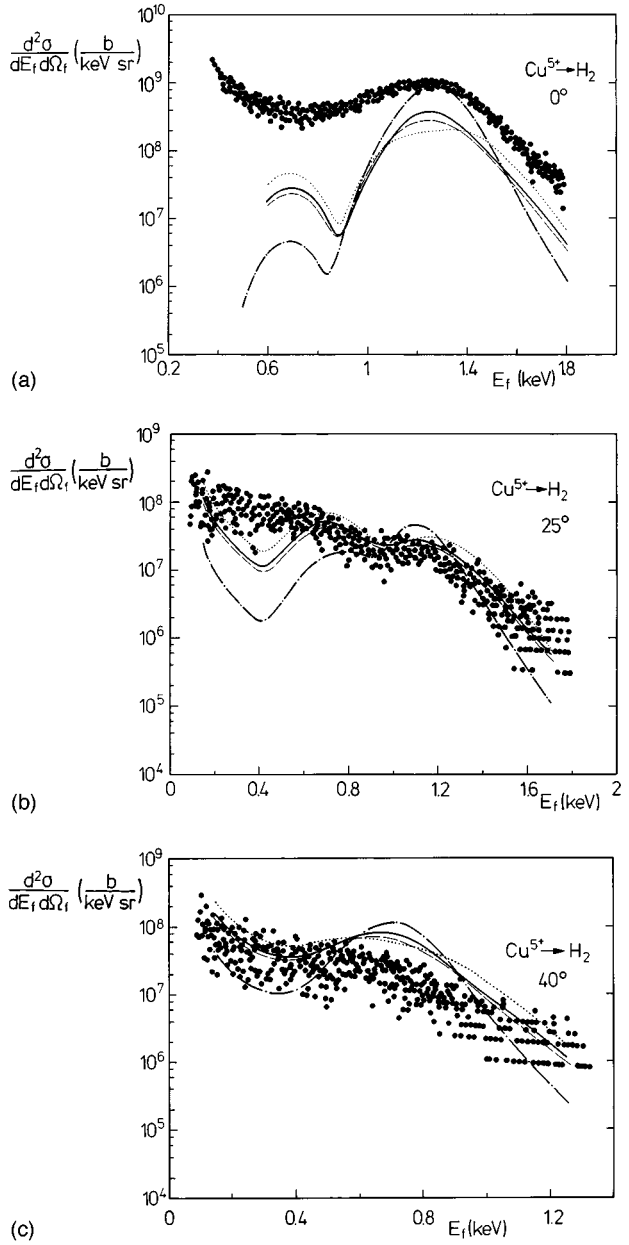

FIG. 2. Doubly differential cross section for electron emission in 0.6 MeV/amu $Cu^{5+}+H_2$ collisions at emissions angles 0° (a), 25° (b), and 40° (c). Experimental data: ●, Wolff *et al.* [10]. Theory: —, *a*-EIA; -·-·-·-, EIA; ···, UA $4d_{3/2}$; ---, $Z_{\text{eff}}=1.61$.

ventional EIA. Part of the difference in intensity between the calculated and the measured spectra may be due to the fact that no coincidence is made with a fixed charge state of the transmitted ions. Therefore, the measured spectra will contain some contribution from projectile ionization that is not considered in theory and that is most serious for forward electron emission.

At the larger angles [Figs. 2(b) and 2(c)], the *a*-EIA results are in considerably better agreement with experiment, both in shape and in intensity. In the 25° spectra, a double-peak structure is visible, which can be traced back to a Ramsauer-Townsend minimum in the elastic e-Cu^{5+} scattering cross section near 120° (in the projectile reference frame [10] corresponding to a laboratory angle of ~30°; see also

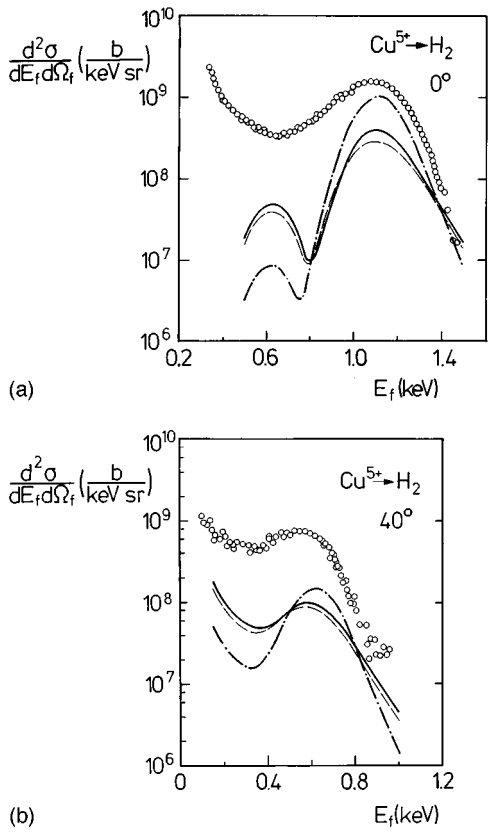

FIG. 3. Doubly differential cross section for electron emission in 0.53 MeV/amu $Cu^{5+}+H_2$ collisions at emission angles 0° (a) and 40° (b). Experimental data: ○, Liao [11]. Theory: —, *a*-EIA; -·-·-·-, EIA; ---, $Z_{\text{eff}}=1.61$.

Fig. 4). While this structure is very pronounced in the EIA results, it is damped in the *a*-EIA results in a similar way as in the measurements.

Figure 3 shows the electron spectra from the Kansas group [11,29] for 0.53 MeV/amu Cu^{5+} on H_2 at 0° and 40°. These data are absolutely measured singles data. The theoretical results for zero degrees compare to experiment in a similar way as in Fig. 2(a). However, the discrepancy in intensity between *a*-EIA and the data persists at the larger angles, being nearly an order of magnitude at 40° [Fig. 3(b)]. Also, the binary-encounter peak is more pronounced than in the 0.6 MeV/amu $Cu^{5+}+H_2$ spectra, such that the decrease of the *a*-EIA results on the high-energy wing of the BE peak is too slow as compared with experiment.

The different behavior of the 0.53 and 0.6 MeV/amu $Cu^{5+}+H_2$ collision systems at the larger angles cannot be ascribed to a dynamical effect since the two collision velocities differ by 6% only. Indeed, the EIA and *a*-EIA results are much alike for the two systems. This suggests some inconsistency in the acquisition of the data of Wolf *et al.* and Hagmann and co-workers. In order to be more specific, the singly (angular) differential cross sections are plotted in Fig. 4, which are obtained upon integrating each spectrum across the binary-encounter peak. The Hagmann and co-workers BE peak yields are available from the experimentalists [11,29] while the 0.6-MeV/amu data points were found from directly integrating the measured spectra [10,30] without any

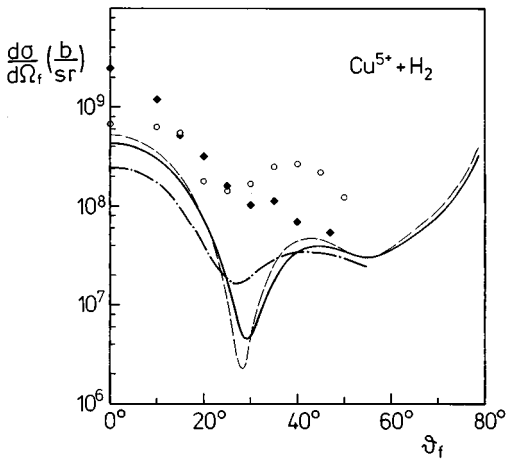

FIG. 4. Singly differential cross section as a function of angle ϑ_f. Experiment: binary-encounter peak yield in 0.6 MeV/amu (◆, Wolff *et al.* [10]) and 0.53 MeV/amu (○, Liao [11]) $Cu^{5+}+H_2$ collisions. Theory: cross section for elastic electron scattering from Cu^{5+} for $k=v=4.9$ (—) and 4.6 (---); binary-encounter peak yield in 0.6 MeV/amu $Cu^{5+}+H_2$ collisions from EIA theory (-·-·-·-·-).

background subtraction procedure. Therefore, the latter data may be systematically too high. It is obvious, however, that the data of Wolf *et al.* fall off by nearly two orders of magnitude when ϑ_f is increased from 0° to 40°, whereas the 0.53-MeV/amu data decrease by less than a factor of 5 and exhibit a distinct second maximum around 40°. In order to stress the relation between BE electron emission and free-electron scattering, we have included in Fig. 4 the elastic-scattering cross section of electrons from Cu^{5+} at $k=v=4.6$ and 4.9 corresponding to the Cu^{5+} collision velocities. This cross section is conveniently calculated in the projectile reference frame [termed $d\sigma'/d\Omega(k,\theta)$, with $\theta=\pi-2\vartheta_f$], and is subsequently transformed to the target reference frame by means of [1]:

$$\frac{d\sigma}{d\Omega_f}=4N_i\cos\vartheta_f\frac{d\sigma'}{d\Omega}(k,\theta), \tag{17}$$

where $N_i=2$ is the number of target valence electrons. At the lower velocity, the Ramsauer-Townsend minimum at 30° is somewhat more pronounced than for $v=4.9$, but otherwise the two cross sections are much alike, confirming the weak velocity dependence of the cross sections discussed earlier. In order to compare with the quasielastic scattering data, the cross section (17) has to be folded with the bound-state momentum distribution as done in the EIA and a-EIA theories. This leads to a considerable damping of the Ramsauer-Townsend structures (for the a-EIA even more than for the EIA), which nevertheless are more easily discernible in the singly differential cross sections than in the BE electron spectra. At angles up to ~35°, the data of Wolf *et al.* are in good accord with the EIA on a relative scale, whereas the shape of the second maximum in the angular distribution is better reproduced by the Kansas data (although these data seem to be substantially too high at the larger angles).

B. Scaling relations and the $Cu^{4+}+H_2$ system

When investigating the test system Cu^{5+} on H, we have found that the initial-state occupation probabilities P_i vary smoothly with v and depend only weakly on impact parameter b. We therefore have tried to fit the P_i to a general formula,

$$\overline{P_i}=\frac{p_i}{\sum_i p_i},\quad p_i=n_i e^{-\beta|\overline{\Delta\varepsilon_i}|^{\mathrm{UA}}/v}, \tag{18}$$

where the inverse velocity dependence in the exponent is suggested by the Landau-Zener formula (15) with (16). In this expression, $\overline{\Delta\varepsilon_i}^{\mathrm{UA}}$ is the mean united-atom energy difference of a group i of levels belonging to the same subshell from the ''central'' UA state, which correlates asymptotically to the occupied target state [for $Cu^{5+}+H$ the $4d$ state, while i runs over $(4p, 4d, 5s, 5p, 5d)$]. The number of subshells in the group i that couple to the central state is denoted by n_i. β is a fit parameter that is found to be $\beta=7.5$ in the case of the average probabilities for $Cu^{5+}+H$ given above. The formula (18), which assumes that the energy difference at the crossing point can be replaced by the corresponding united-atom energy difference, and that the adiabatic coupling matrix elements are much alike, makes detailed knowledge of correlation diagrams and coupling strengths unnecessary. It is only required to know the ''central'' UA state, i.e., to which UA state the initial state of the active target electron is correlating.

The basic importance of this central UA state suggests an even simpler approximation to the a-EIA formula. Instead of summing over the momentum-space densities of the true UA states with weighting factors P_i, one might simply take one ''averaged'' bound-state density instead. We have included in Figs. 2 and 3 the results for the choice of a single $1s$-type hydrogenic state with an effective charge $Z_{\mathrm{eff}}=\sqrt{2|\varepsilon_c|^{\mathrm{UA}}}$ calculated from the binding energy $|\varepsilon_c|^{\mathrm{UA}}$ of the central UA state [the $(Cu^{5+}+H)$ $4d_{3/2}$ UA state energy results in $Z_{\mathrm{eff}}=1.61$]. In all cases, these results are surprisingly close to those from the a-EIA theory. For the sake of comparison, we show in Fig. 2 also results where in the a-EIA formula (6) solely the central UA state has been included with $P_i=1$. It is seen that only for $\vartheta_f=25°$ does the energy dependence follow the a-EIA theory, but for the other two angles, the resulting BE peak is considerably broader and lower in intensity than predicted by the a-EIA theory. This indicates that structures or peculiarities in the BE peak region of the electron spectra arising from the nodal structure of particular UA wave functions contributing to the cross section (6) are largely averaged out by calculating the weighted sum over all relevant states, such that the resulting momentum space density resembles the density of an occupied atomic shell (and is therefore of $1s$ type).

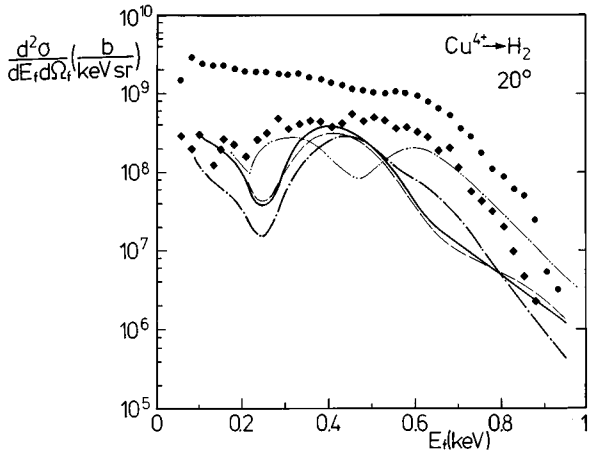

FIG. 5. Doubly differential cross section for electron emission in 0.3 MeV/amu $Cu^{4+}+H_2$ collisions at $\vartheta_f=20°$. Experimental data from Liao [11]: ●, singles data; ◆, data in coincidence with transmitted Cu^{4+}. Theory: —, a-EIA; -·-·-·-, EIA; ---, $Z_{\rm eff}=1.68$ (present calculations); -·-·-·-·-·-, peaked EIA from Bhalla (as quoted in Liao [11]).

As an application of the scaling relations discussed above, we show in Fig. 5 results for the collision system 0.3 MeV/amu $Cu^{4+}+H_2$ in comparison with experiment [11,29]. Both singles data and data in coincidence with transmitted Cu^{4+} projectiles are measured on an absolute scale. These data indicate that projectile ionization can be quite important (Cu^{4+} being of course more easily ionized than Cu^{5+}), giving a similar contribution to the BE peak yield as pure target ionization at the considered angle of 20°. The very broad experimental BE peak at this angle is again caused by the influence of Ramsauer-Townsend structures. Pronounced double-peak structures are visible in the (peaked) EIA calculations of Bhalla [9,13] included in Fig. 5, but they are largely damped out in our (unpeaked) EIA results. We also show a-EIA results from Eq. (6) with P_i approximated by Eq. (18), assuming that the collision system under investigation is sufficiently close to the 0.53–0.6 MeV/amu $Cu^{5+}+H$ systems such that the scaling relations are supposed to give reliable results (with β unchanged). With the help of the LCAO-MO basis set method we have found that the occupied target electronic state correlates to the UA-$4p_{3/2}$ state (with energy -38.22 eV), which actually is the one closest in energy to the central UA $4d_{3/2}$ state of the $Cu^{5+}+H$ system (at -35.41 eV). This could be an indication that the energy of the central UA state depends only weakly on the projectile. In contrast, its dependence on the target (for $Z_P \gg Z_T$) is much stronger according to LCAO-MO calculations for $Cu^{5+}+He$ where the central state is the UA $4s_{1/2}$ state (with energy -68.45 eV).

Besides the a-EIA calculation, we have plotted in the figure results for the choice of a single hydrogenic $1s$ state with $Z_{\rm eff}=1.68$ corresponding to the UA $4p_{3/2}$ binding energy. Again, both calculations give very similar results. However, none of the theories is able to correctly account for the measured BE peak shape, and not even the a-EIA model provides any particular improvement for this collision system.

IV. CONCLUSION

Binary-encounter-electron emission from collisions with medium-energy, highly charged projectiles has been calculated within an adiabatic binary-encounter model where the initial-state occupation probabilities of the individual molecular orbitals have been found from an LCAO-MO calculation combined with the Landau-Zener formalism. For the test system $Cu^{5+}+H$ we were able to deduce scaling relations that allow for an approximate determination of the initial-state occupation numbers solely from the knowledge of the united-atom level diagram and of the ''central'' UA level to which the active target electron is correlating. Even more, we have found that our results for the doubly differential cross section for BE electron emission are in many cases well approximated by applying a very simplified prescription. This consists in using the conventional electron-impact approximation with one hydrogenlike initial $1s$ state for each active target electron characterized by an effective charge. The charge parameter $Z_{\rm eff}$ is determined from the energy $\varepsilon_c^{\rm UA}$ of the central UA state. This prescription works because in the a-EIA calculations one must sum over many levels, hence damping out most of the wave-function effects. For all models it is therefore crucial to know the central UA state or rather its energy for a given projectile ion-target combination. Assuming that the projectile dependence of this energy is weak for a given target, one may apply the simplified model to other collision systems without knowledge of the corresponding correlation diagram.

The comparison of our theory with experimental data is hampered by the fact that the data sets from two experimental groups are not internally consistent. The data from the Schmidt-Böcking group rapidly decrease in intensity upon increasing the electron ejection angle and show a very broad BE peak. This characteristic is observed for a great variety of projectiles [10,30] colliding with H_2 or He. Our adiabatic model is quite successful in explaining the relative energy dependence of the BE electrons for not too high collision velocities even for other projectiles like Xe^{21+} colliding with He (using the simplified one-state prescription). On the other hand, the spectra from Hagmann and co-workers show a sharp BE peak even at the higher angles, and the peak intensity decreases only very slowly with angle. For many of these spectra, our a-EIA theory overestimates the peak width on the high-energy wing and dramatically underpredicts the electron intensity. Further independent experiments are necessary to clarify the situation.

ACKNOWLEDGMENTS

We would like to thank S. Hagmann as well as W. Wolff and H. Wolf for the communication of experimental data and for many discussions, and P. A. Amundsen for providing the fast Bessel transform routine. Financial support from the Deutsche Forschungsgemeinschaft (DFG), GSI Darmstadt, the Division of Chemical Sciences, Office of Basic Energy Sciences, Office of Energy Research, and U.S. Department of Energy is gratefully acknowledged.

[1] M. W. Lucas, D. H. Jakubassa-Amundsen, M. Kuzel, and K. O. Groeneveld, Int. J. Mod. Phys. A **12**, 305 (1997).
[2] P. Richard, D. H. Lee, T. J. M. Zouros, J. M. Sanders, J. L. Shinpaugh, and H. Hidmi, J. Phys. B **23**, L213 (1990).
[3] S. Hagmann, C. Liao, C. Bhalla, R. Shingal, J. Shinpaugh, W. Wolff, H. Wolf, R. Mann, and R. Olson, Radiat. Eff. Defects Solids **126**, 35 (1993).
[4] R. D. DuBois, L. H. Toburen, M. E. Middendorf, and O. Jagutzki, Phys. Rev. A **49**, 350 (1994).
[5] C. Liao, P. Richard, S. R. Grabbe, C. P. Bhalla, T. J. M. Zouros, and S. Hagmann, Phys. Rev. A **50**, 1328 (1994).
[6] M. Sataka, M. Imai, Y. Yamazaki, K. Komaki, K. Kawatsura, Y. Kanai, H. Tawara, D. R. Schultz, and C. O. Reinhold, J. Phys. B **27**, L171 (1994).
[7] C. Kelbch, S. Hagmann, S. Kelbch, R. Mann, R. E. Olson, S. Schmidt, and H. Schmidt-Böcking, Phys. Lett. A **139**, 304 (1989).
[8] S. Hagmann, W. Wolff, J. L. Shinpaugh, H. E. Wolf, R. E. Olson, C. P. Bhalla, R. Shingal, C. Kelbch, R. Herrmann, O. Jagutzki, R. Dörner, R. Koch, J. Euler, U. Ramm, S. Lencinas, V. Dangendorf, M. Unverzagt, R. Mann, P. Mokler, J. Ullrich, H. Schmidt-Böcking, and C. L. Cocke, J. Phys. B **25**, L287 (1992).
[9] W. Wolff, J. L. Shinpaugh, H. E. Wolf, R. E. Olson, J. Wang, S. Lencinas, D. Piscevic, R. Herrmann, and H. Schmidt-Böcking, J. Phys. B **25**, 3683 (1992).
[10] W. Wolff, J. Wang, H. E. Wolf, J. L. Shinpaugh, R. E. Olson, D. H. Jakubassa-Amundsen, S. Lencinas, U. Bechthold, R. Herrmann, and H. Schmidt-Böcking, J. Phys. B **28**, 1265 (1995).
[11] C. Liao and S. Hagmann (unpublished); C. Liao, thesis, Kansas State University, 1995 (unpublished).
[12] D. Banks, L. Vriens, and T. F. M. Bonsen, J. Phys. B **2**, 976 (1969).
[13] D. H. Jakubassa, J. Phys. B **13**, 2099 (1980).
[14] D. R. Schultz and R. E. Olson, J. Phys. B **24**, 3409 (1991).
[15] C. P. Bhalla and R. Shingal, J. Phys. B **24**, 3187 (1991).
[16] J. Wang, C. O. Reinhold, and J. Burgdörfer, Phys. Rev. A **44**, 7243 (1991).
[17] U. Wille and R. Hippler, Phys. Rep. **132**, 129 (1986).
[18] W.-D. Sepp, D. Kolb, W. Sengler, H. Hartung, and B. Fricke, Phys. Rev. A **33**, 3679 (1986).
[19] P. Kürpick, W.-D. Sepp, and B. Fricke, J. Phys. B **24**, L139 (1991).
[20] P. Kürpick, W.-D. Sepp, and B. Fricke, Phys. Rev. A **51**, 3693 (1995).
[21] N. F. Mott and H. S. W. Massey, *The Theory of Atomic Collisions* (Clarendon, Oxford, 1965), Sec. XXI, Subsec. 5.
[22] A. Salop and R. E. Olson, Phys. Rev. A **13**, 1312 (1976).
[23] J. S. Briggs, J. Phys. B **10**, 3075 (1977).
[24] D. H. Jakubassa-Amundsen, Z. Phys. D **34**, 9 (1995).
[25] H. M. Hartley and H. R. J. Walters, J. Phys. B **20**, 3811 (1987).
[26] F. A. Gianturco and S. Scialla, J. Phys. B **20**, 3171 (1987).
[27] J. D. Talman, J. Comput. Phys. **29**, 35 (1978).
[28] P. A. Amundsen (private communication).
[29] S. Hagmann (private communication).
[30] H. Wolf and W. Wolff (private communication).